

**Effects of Alpha Particle Stopping-Power Models
on Inertial Confinement Fusion Implosions**

Nathan Xu

Pittsford Sutherland High School, 55 Sutherland Street, Pittsford, NY, 14534

Advisor: Dr. S. X. Hu

Laboratory for Laser Energetics, University of Rochester, Rochester NY

October 2014

Abstract

An important issue in the design of inertial confinement fusion (ICF) implosion experiments is calculating the proper energy-deposition rate of the alpha particles as they travel through the plasma. In this project, four different models of stopping power (energy deposition), based on different physics approximations, have been examined: the Skupsky model (currently used in Laboratory for Laser Energetics' hydrocodes), the Li-Petrasso model, the quantum molecular dynamics model, and the Brown-Preston-Singleton model. These models have been tested for different deuterium-tritium (DT) plasma conditions such as temperature, density, and initial alpha particle energy. The models have been implemented into the one-dimensional hydrocode *LILAC*, allowing their effects on National Ignition Facility-scale ignition implosions to be investigated. Contrary to what was expected, the results show significant differences in the overall target performance depending on which model is used; differences in target gain vary by a factor of two. Finally, an experiment has been suggested to verify which model, if any, is truly valid.

1. Introduction

Around the world, nuclear fusion, a virtually inexhaustible source of power, has been studied for the past few decades. Inertial confinement fusion (ICF), using powerful lasers, is one way to make nuclear fusion a viable clean energy source [1]. During laser-driven ICF implosion experiments, laser pulses ablate the surface of a layered target and implode the target through the “rocket” effect [2]. The target is a spherical plastic capsule (Figure 1a) with a layer of deuterium-tritium (DT) ice, and filled with DT gas. The powerful laser-driven shocks and the spherical convergence, as shown in Figure 1b, compress the DT, creating extreme temperatures and pressures. The high temperatures and densities cause the DT to fuse together to produce energetic alpha (α) particles and neutrons ($D+T=\alpha+n+17.6$ MeV). The alpha particle is created with an energy of 3.54 MeV.

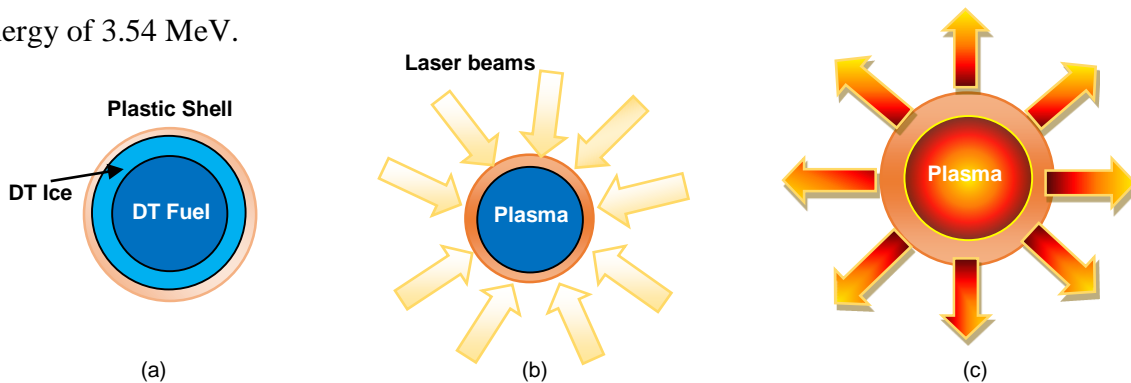


Figure 1: Illustration of the direct-drive ICF implosion

(a) The target is a spherical plastic capsule 1 to 3 mm in diameter; (b) The fuel target is compressed by the implosion of the hot surface material caused by laser shocks; (c) The compressed hot fuel core ignites and the “bootstrapping” process occurs. Thermonuclear burn spreads, yielding many times the input energy.

The implosion generates a relatively low-temperature and high-density shell and a high-temperature and medium-density hotspot center. The alpha particles that are created from the reaction in the target center carry the energy that is necessary to further heat DT plasmas for more fusion reactions to occur, which is called a “bootstrapping” process. This “bootstrapping” process eventually leads to ignition and energy gain. Ignition is when output energy equals input energy or gain = 1; gain is the ratio of output energy to input energy.

As the positively charged alpha particles travel through the plasma, they deposit their energies; the neutrons do not deposit a significant amount of energy in the plasma because neutrons are uncharged and marginally influenced by the plasma. Stopping power, the rate at which energy is transferred from the alpha particles back to the plasma, is directly involved in determining the

effectiveness of the “bootstrapping” process. In ICF simulation codes, stopping power is calculated by using a physics model that approximates the interaction process between traveling particles (i.e., alpha particles) and matter (i.e., the plasma). Several stopping power models have been proposed.

One of the purposes of this study is to evaluate four proposed models of stopping power in the one-dimensional simulation code *LILAC* currently used for ICF implosion experiments at the Laboratory for Laser Energetics (LLE), University of Rochester. The four models are the Brown-Preston-Singleton (BPS) model [3], the Li-Petrasso (LP) model [4], the Skupsky model [5], and the Quantum Molecular Dynamics (QMD) model [6]. The Skupsky model is currently used in the hydro-code *LILAC* [7]. In this study, the other three models were implemented into *LILAC* in order to estimate the stopping power in different DT plasma conditions such as temperature, density, and initial alpha particle energy. A comparison of results was performed to show the variations among the four models. Contrary to what was expected, the results show significant differences in the overall target performance depending on which model is used; differences in target gain varied by a factor of two. Finally, an experiment has been suggested to verify which model, if any, is truly valid.

The paper is organized as follows: In Section 2, the four stopping power models are described. In Section 3, results are presented for the comparisons of these four models. The stopping power effects are examined in hydro-simulations in Section 4. In Section 5, a future experiment to test the four models in measurable plasma conditions is suggested. Finally, a conclusion is presented in Section 6.

2. Models of Stopping Power

2.1. Stopping Power

Stopping power describes the rate of energy loss by charged particles or the energy deposited in the matter. It can be expressed in a generic formula as shown in equation 2.1.1.

$$S(E) = -dE/dx \quad 2.1.1$$

The stopping power, $S(E)$, of the matter is equal to the loss of energy E per unit path length, x . The mean travel range of the particle, Δx , can be calculated by integrating the reciprocal stopping power over energy shown in equation 2.1.2.

$$\Delta x = \int_0^{E_0} \frac{1}{S(E)} dE \quad 2.1.2$$

where E_0 is the initial kinetic energy of the particle. The total deposited energy can be obtained by integrating the stopping power over the entire path length of the particle while it moves in the matter.

In plasma physics, stopping power is defined as the retarding force acting on charged particles due to interaction with matter, resulting in loss of particle energy [8]. In the beginning of the slowing-down process at high energies, the charged particle is slowed down mainly by electrons and moves in a nearly straight path. When the particle has slowed down sufficiently, its collisions with ions dominate the slowing down process while its path becomes more erratic [9]. In direct-drive ICF implosion experiments, an alpha particle from DT fusion encounters various conditions while traveling from the hot spot center towards the outside, e.g., hot and cold temperatures and low and high densities [2]. When the DT fuel absorbs enough α -particle energy so that the plasma temperature increases, more fusion reactions are started and the burn process begins. The stopping power determines the number of subsequent fusion reactions that occur within the target. Thus, the stopping power is directly involved in determining the energy output. The stopping power of a particle depends on the temperature and density of the matter and the energy of the particle passing through the matter.

2.2. Models of Stopping Power

The stopping power of a charged particle is usually attributed to two major types of interactions between the charged particle and the plasma: electron and ion stopping power. Electron stopping power refers to the slowing down of a traveling ion due to inelastic collisions between bound electrons in the matter and the ion moving through it. Ion stopping power refers to the elastic collisions between the traveling ion and ions in the plasma. The interaction between the ions and plasma is a rather complex process. It is very difficult to describe all possible interactions for all possible ion charge states. Analytic models have been proposed based on these major interactions under certain assumptions. For example, a Coulomb logarithm is used in each model discussed below to model the Coulomb interactions between charged particles. The Coulomb logarithm is a unit-less parameter fundamental to many plasma properties; it helps to determine charged particle stopping in the plasma.

These models differ to some degree in their assumptions. These assumptions are often related to the condition of the plasma. For example, the differing physics assumptions of each model affect the pre-factor and parameters used in the Coulomb logarithm.

A. *Brown-Preston-Singleton (BPS) model*

Brown, Preston and Singleton introduced the BPS model in 2005 [3]. The BPS model utilizes the dimensional continuation method, which is related to the quantum mechanical description of dense plasmas, to compute the energy loss rate for a non-relativistic particle moving through fully ionized plasma. The model worked out a formula for the electron-ion energy transfer rate in a wide range of plasma conditions including quantum and coupling effects. The BPS model puts no restriction on the charge, mass, or speed of a particle. It assumes that the plasma is not strongly coupled in the sense that the dimensionless plasma coupling parameter is small.

The total stopping power for BPS is the sum of the following two formulas:

$$\frac{dE_p}{dx} = \frac{e_p^2 \omega_b^2}{4\pi v_p^2} (\ln \Lambda) \quad 2.2. A1$$

$$\frac{dE_p}{dx} = \frac{e_p^2}{4\pi} \kappa_e^2 (\ln \Lambda) \frac{2}{3} \left(\frac{\beta m_e v_p^2}{2\pi} \right)^{\frac{1}{2}} \quad 2.2. A2$$

where the ionic plasma frequency is $\omega_b^2 = 4\pi e_b^2 n_b / m_b$, n_b is the ion density, m_b is the ion mass, m_e is the electron mass, e_b is the background ion charge, e_p and v_p are the charge and velocity of the projectile particle, $\ln \Lambda$ is the Coulomb logarithm, β is $1/k_B T$, k_B is the Boltzmann constant, and κ_e is the electron Debye wave number. Subscript p is used when describing the projectile particle; subscript b is used when describing the background plasma ions. Equation 2.2.A1 gives the stopping power due to ions and equation 2.2.A2 gives the stopping power due to electrons.

The Coulomb logarithm $\ln \Lambda$ in the BPS model is comprised of three terms [3], a main term and two correction factors, shown here:

$$\ln \Lambda_{BPS} = \ln \Lambda_{BPS}^{QM} + \ln \Lambda_{BPS}^{\Delta C} + \ln \Lambda_{BPS}^{FD} \quad 2.2. A3$$

The leading term incorporates quantum mechanics effects, while the second term is a correction for the case where the plasma coupling parameter is no longer near the quantum limit; the third term takes the many-body electron degeneracy effect into account when Fermi-Dirac statistics become relevant. Each term, ignoring small electron-ion mass ratio effects, is given as:

$$\ln \Lambda_{BPS}^{QM} = \frac{1}{2} \left[\ln \left(\frac{8k_B^2 T_e^2}{\hbar^2 \omega_e^2} \right) - \gamma - 1 \right] \quad 2.2. A3.1$$

$$\ln \Lambda_{BPS}^{\Delta C} = \frac{e_H}{k_B T_e} \sum_i \frac{\omega_i^2 Z_i^2}{\omega_i^2} \left\{ 1.20205 \left[\ln \left(\frac{k_B T_e}{Z_i^2 e_H} \right) - \gamma \right] + 0.39624 \right\} \quad 2.2. A3.2$$

$$\ln \Lambda_{BPS}^{FD} = \frac{n_e \lambda_e^3}{2} \left\{ -\frac{1}{2} \left(1 - \frac{1}{2^{3/2}} \right) \times \left[\ln \left(\frac{8k_B^2 T_e^2}{\hbar^2 \omega_e^2} \right) - \gamma - 1 \right] + \left(\frac{\ln 2}{2} + \frac{1}{2^{5/2}} \right) \right\} \quad 2.2. A3.3$$

where e_H is the binding energy of hydrogen, $\hbar = h/2\pi$, h is the Planck constant, Z_i is the effective charge number, n_e is the electron density, and γ is the Euler constant (0.57721). The electron and ion plasma frequencies are given by ω_e and ω_i , respectively; ω_l is the average ion frequency. The BPS model also includes the electron thermal wavelength, λ_e [3].

B. Li-Petrasso (LP) model

Li and Petrasso proposed their analytic model for charged-particle stopping powers for inertial confinement fusion plasmas in 1993[4]. Previously, ion stopping power for large-angle scattering was not considered or treated properly in the analytic models. Collective plasma effects were ignored and the plasma Fokker-Planck equation was limited to an upper limit. The LP model includes important effects, such as plasma ion stopping effects, collective plasma oscillation effects, and quantum effects. The LP model also generalizes the use of the Fokker-Planck equation, which properly treats the effects of large-angle scattering as well as small-angle collisions[4]. It was the first time that the effects of scattering had been properly treated in the calculation of charged-particle stopping power in inertial confinement fusion plasmas.

The LP stopping power formula for test particles (t) by field particles (f) is

$$\frac{dE_{(t,f)}}{dx} = -\frac{(Z_t e)^2}{v_t^2} \omega_{pf}^2 G\left(x^{\bar{f}}\right) \ln \Lambda_b \quad 2.2.B1$$

where $G\left(x^{\bar{f}}\right)$ is given by

$$G\left(x^{\bar{f}}\right) = \mu\left(x^{\bar{f}}\right) - \frac{m_f}{m_t} \left\{ \frac{d\mu\left(x^{\bar{f}}\right)}{dx^{\bar{f}}} - \frac{1}{\ln \Lambda_b} \left[\mu\left(x^{\bar{f}}\right) + \frac{d\mu\left(x^{\bar{f}}\right)}{dx^{\bar{f}}} \right] \right\} \quad 2.2.B2$$

$$x^{\bar{f}} = v_t^2 / v_f^2 \quad 2.2.B2.1$$

$$v_f^2 = \frac{2k_B T_f}{m_f} \quad 2.2.B2.2$$

$$\omega_{pf} = (4\pi n_f e_f^2 / m_f)^{1/2} \quad 2.2.B2.3$$

$$\mu\left(x^{\bar{f}}\right) = 2 \int_0^{x^{\bar{f}}} \frac{e^{-\xi} \sqrt{\xi} d\xi}{\sqrt{\pi}} \quad 2.2.B2.4$$

The Coulomb logarithm is given by

$$\ln \Lambda_b = \ln \left(\frac{\lambda_D}{p_{min}} \right) \quad 2.2.B3$$

$$p_{min} = [p_{\perp}^2 + (h/2m_r u)^2]^{1/2} \quad 2.2.B3.1$$

$$p_{\perp} = e_t e_f / m_r u^2 \quad 2.2.B3.2$$

$$m_r = (m_t m_f) / (m_t + m_f) \quad 2.2.B3.3$$

The constants are defined here: $Z_t e$ is the test charge, e is the electron charge, v_t (v_f) is the test (field) velocity, m_t (m_f) is the test (field) mass, w_{pf} is the field plasma frequency, $\mu(x^{t/f})$ is the Maxwell integral; λ_D is the Debye length, m_r is the reduced mass and u is the relative velocity, n_t (n_f) is the test (field) density, e_t (e_f) is the test (field) charge. Test parameters are similar to projectile particle parameters and field parameters are similar to plasma parameters.

C. Skupsky model

Skupsky [5] was the first to examine the Coulomb logarithm for inverse-bremsstrahlung laser absorption for plasmas of different ionic charge, spanning the classical and quantum-mechanical limits. Previously, this term had not been calculated exactly for the conditions of interest in laser fusion experiments; it had only been estimated from physical considerations.

For short-wavelength irradiation (e.g., 0.35 μm), uncertainties in the ‘‘logarithmic’’ factor can produce variations of 20–50 % in the laser absorption coefficient. A more exact treatment of this term is presented here. For low- Z plasmas, a modified approximation is used that reproduces previous results for long-range interactions that cannot be described by a single electron-ion collision, and it simultaneously treats the short-range electron-ion encounters. For high- Z plasmas, the Coulomb logarithm is calculated in terms of the classical, nonlinear electron trajectory in a self-consistent electrostatic potential; strong ion-ion correlations are treated by the nonlinear Debye-Hückel model.

$$\frac{dW}{dx} = -\sqrt{W} n_e \frac{Z^2 e^4}{(k_B T)^{\frac{3}{2}}} \left(\frac{m_e}{M}\right)^{\frac{1}{2}} \sqrt{\pi} \frac{8}{3} \left(\frac{\sqrt{\pi}}{2F_{\frac{1}{2}}(\eta) e^{-\eta} + 1} \right) \ln \Lambda_{RPA} \quad 2.2.C1$$

where $F_{\frac{1}{2}}(\eta)$ is the Fermi integral

$$F_{\frac{1}{2}}(\eta) = \frac{1}{\Gamma(\frac{3}{2})} \int_0^{\infty} \frac{t^{\frac{1}{2}}}{e^{t-\eta} + 1} dt \quad 2.2.C2$$

and where the Coulomb logarithm is defined as

$$\ln \Lambda_{RPA} = (1 + e^{-\eta}) \int_0^{\infty} d\kappa \frac{\kappa^3}{(\kappa^2 + \kappa_0^2)^2} \left[\exp\left(\frac{\hbar^2 \kappa^2}{8m_e k_B T}\right) - \eta \right]^{-1}. \quad 2.2.C3$$

Equation 2.2.C1 is simplified into

$$\frac{dW}{dx} = \frac{Z^2 e^2}{2\pi^2 v_0} \int \frac{d\vec{\kappa}(\vec{\kappa} \cdot \vec{v}_0)}{\kappa_D^2} \text{Im} \frac{1}{\epsilon(\vec{\kappa}, \vec{\kappa} \cdot \vec{v}_0)} \quad 2.2.C4$$

$$\epsilon(\vec{k}, \vec{k} \cdot \vec{v}_0) = 1 + \sum_s \frac{4\pi Z_s^2 e^2}{m_s \kappa_D^2} \int d\vec{v} \frac{\vec{k} \cdot \partial f_s / \partial \vec{v}}{\omega - \vec{k} \cdot \vec{v}_0 + i\delta} \quad 2.2. C5$$

where W is the particle energy, n_e is the electron number density, Z_s is the background ion charge, Z is the charge of the particle projectile, \vec{v}_0 is the velocity, κ is the wave number of plasma electrons, η is the electron degeneracy parameter, f_s is the Fermi-Dirac single-particle distribution function, $\kappa_0^2 = \kappa_D^2 F_1'(\eta) / F_1(\eta)$, κ_D is the Debye wave number, and $\kappa_D^2 = 4\pi n_e e^2 / k_B T$.

D. Quantum Molecular Dynamics (QMD) model

The QMD model is the same as the Skupsky model except that its Coulomb logarithm is replaced by the QMD-calculated one and the model considers many-body physics [6]. This means that the interactions between charged particles take into account all of a particle's nearby surroundings, rather than just the two particles directly involved in the collision.

The QMD stopping power is given by

$$\frac{dW}{dx} = -\sqrt{W} n_e \frac{Z_{\text{eff}}^2 e^4}{(k_B T)^2} \left(\frac{m_e}{M}\right)^{\frac{1}{2}} \sqrt{\pi} \frac{8}{3} \left(\frac{\sqrt{\pi}}{2F_{\frac{1}{2}}(\eta)} \frac{1}{e^{-\eta} + 1}\right) \times (\ln\Lambda)_{\text{QMD}} \quad 2.2. D1$$

$$(\ln\Lambda)_{\text{QMD}} = \exp\left\{\alpha_0 + \sum_{i=1}^5 \left[\alpha_i (\ln\Gamma)^i + \beta_i (\ln\theta)^i\right]\right\} \quad 2.2. D2$$

where Z_{eff} is the effective charge number, $\theta = T/T_F$ is the degeneracy parameter (T_F is the Fermi temperature) and the values of α_i and β_i in $\ln\Lambda_{\text{QMD}}$ are listed in Table 1.

i	α_i	β_i
0	-0.74014809257279	
1	-0.18145905042211	+0.861554200945883
2	+6.39644338111 x 10 ⁻⁴	-0.105703692158405
3	+1.47954277819 x 10 ⁻³	-6.757828681522 x 10 ⁻³
4	-1.23361568162 x 10 ⁻⁴	-1.690070651236 x 10 ⁻⁴
5	-2.58107191013 x 10 ⁻⁵	+3.492008487199 x 10 ⁻⁴

Table 1 The values of α_i and β_i used in the QMD model

3. Comparison of the Stopping Power Models

Within these equations, variables such as temperature, plasma density, and initial energy of a projectile can be varied to model different mediums. Each model was run through a simulation

code, with ICF-relevant electron and ion temperatures and plasma densities, to calculate the stopping power from each model as well as the distance traveled by an alpha particle starting with 3.54 MeV of energy. The greater the alpha particle distance traveled, the less the average stopping power. The most optimistic model for each specific condition is the model that predicts that the distance traveled by the alpha particle is the smallest; in other words, the alpha particle energy is deposited closer to the DT fuel (in the center).

3.1 Stopping Power in Hot Spot Plasma Condition

First, the stopping power was calculated from each of the four models at different alpha particle energy levels (0 to 3.54 MeV) in the plasma at a low DT density of 50 g/cc and a high temperature of 6000 eV. Note that the 3.54 MeV is the normal birth energy of alpha particles created by DT fusion and it is usually used as a starting energy for alpha particles in ICF implosion simulations. The models were compared for the stopping power of alpha particles traveling in the hot spot plasma. The stopping power (dE/dx) is calculated and plotted as a function of initial alpha particle energy as shown in Figure 2. In addition, the decrease of energy with distance traveled is plotted for an alpha particle with initial energy 3.54 MeV.

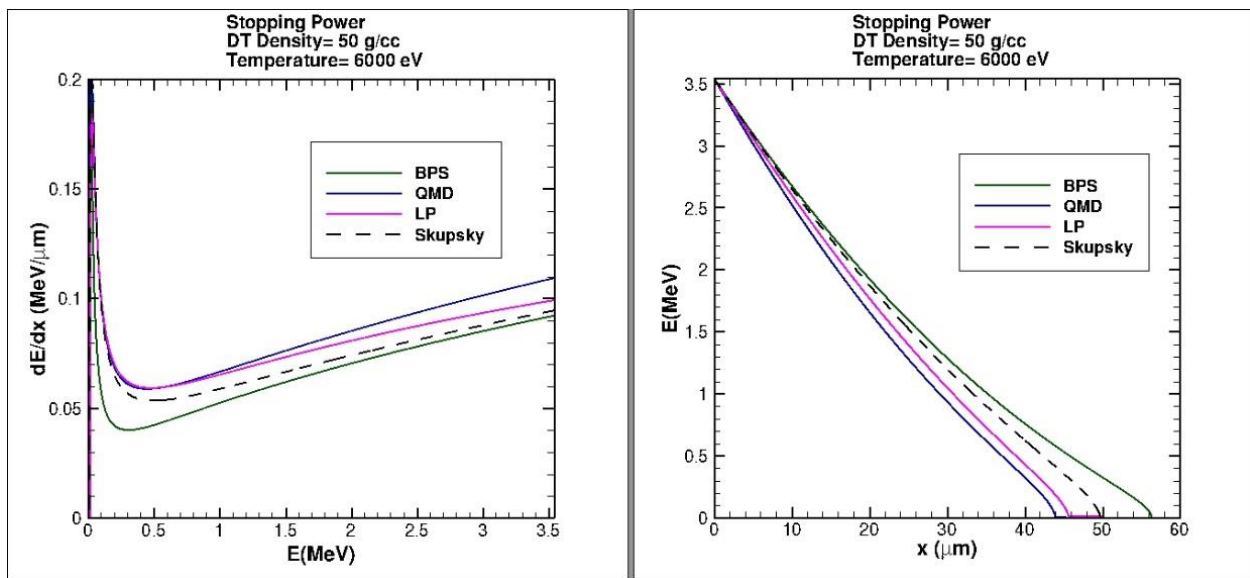


Figure 2: Stopping power calculated in the low-density and high-temperature plasma condition
 The stopping power is plotted as a function of alpha particle energy in the left panel. The right panel shows how far the alpha particle will travel in the hot spot plasma. The two figures are related in that the higher stopping power means a shorter distance traveled.

As shown in Figure 2, there is not much variation between the four models for stopping power or alpha particle distance traveled when the DT density is 50 g/cc and the temperature is 6000 eV. In hot spot DT-plasma conditions, the stopping power can vary by a maximum of 19% among the four models at a particle energy level of 3.54 MeV as shown in Figure 2.

3.2 Stopping Power in Lower Temperature and Dense Plasma Condition (DT shell)

The stopping power was also calculated from each of the four models at different energy levels (0 to 3.5 MeV) in the plasma at a higher DT density (400 g/cc) and a lower temperature (1000 eV). This combination of temperature and density simulates conditions similar to those of the DT shell.

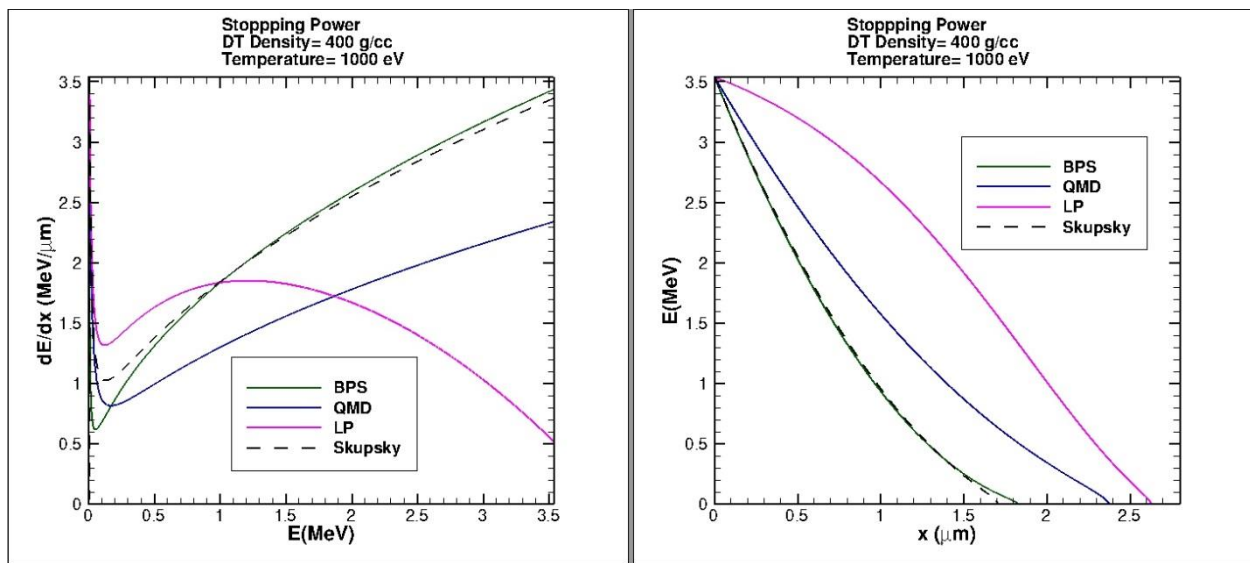


Figure 3: Calculated stopping power in a low temperature and high density plasma condition
 Stopping power is plotted as a function of alpha particle energy in the left panel. The right panel shows how far the alpha particle will travel in low temperature and dense plasma conditions. The two are related in that the higher stopping power means a shorter distance traveled.

The variations among the four models for stopping power and alpha particle distance traveled are rather significant for a low temperature and dense plasma condition as shown in Figure 3. The BPS and Skupsky models yield similar results for the stopping power at all energy levels. The stopping power calculated from the BPS model (3.4 MeV/μm) is roughly seven fold greater than the LP model stopping power (0.5 MeV/μm) when the alpha particle energy is 3.54 MeV. The right panel of Fig. 3 shows that the alpha particle distances traveled as calculated by the four

models vary from 1.7 μm to 2.6 μm . The Skupsky model predicted the smallest distance, making it the most optimistic model for these DT shell conditions.

In general, the stopping power decreases and the distance traveled by an alpha particle increases as the temperature increases. The opposite is true as the density increases, when the stopping power increases and the distance traveled by an alpha particle decreases. An increase in the stopping power leads to more energy being deposited closer to the DT fuel in the center, which allows more fusion reactions to occur.

Some interesting results are found from careful inspection of the stopping power models. First, the models are affected differently by changes in the initial energy of alpha particles, as seen in Figures 2 and 3. Second, a comparison of the figures shows that the order of the stopping power models in terms of the distance traveled from the least to greatest changes when the plasma conditions (temperature and density) are changed.

	% change in distance traveled Temperature (300eV \rightarrow 1000 eV)		% change in distance traveled Temperature (1000 eV \rightarrow 5000 eV)	
	Density= 400 g/cc	Density= 1000 g/cc	Density=400 g/cc	Density=1000 g/cc
BPS	4450	8525.0	339.6	455.1
QMD	17.5	45.5	152.1	71.3
LP	-	-	151.9	-
Skupsky	486.2	1100.0	233.6	275.0

Table 2 Percent change in the distance traveled by an alpha particle at the conditions of plasma density at 400 g/cc and 1000 g/cc when the temperature changes from 300 eV to 1000 eV and from 1000 eV to 5000 eV, respectively. The percent change of distance traveled by an alpha particle as shown in this table is positive.

Tables 2 and 3 show the change (%) in distance traveled by an alpha particle when the temperature and density change. Table 2 shows the change in distance when the temperature changes from 300 to 1000 eV and from 1000 to 5000 eV at 400 g/cc and 1000 g/cc, respectively. The BPS and Skupsky models are affected more by temperature than the QMD model.

	% change in distance traveled Density (400 g/cc→1000 g/cc)	% change in distance traveled Density (400 g/cc→1000 g/cc)
	Temperature= 5000 eV	Temperature= 1000 eV
BPS	-52.1	-62.1
QMD	-54.7	-32.7
LP	-46.8	-
Skupsky	-53.3	-50.6

Table 3 Percent change in the distance traveled by an alpha particle at the temperature conditions of 5000 eV and 1000 eV, respectively, when the plasma density changes from 400 g/cc to 1000 g/cc. The percent changes for both conditions as shown in this table are negative changes (decreases).

At a temperature of 5000 eV, a density change as shown in Table 3 appears to affect all the models similarly; all models have about a 50% decrease in distance traveled. However, at a temperature of 1000 eV, the QMD model predicts a distance traveled that differs from the other models, which appear to be grouped together. The LP model only produces results for low DT density and high temperature conditions. There were many cases in Tables 2 and 3 where the LP model did not produce any data, indicating that the conditions were not applicable to the LP equation.

Overall, it appears that the alpha particle distance traveled is more sensitive to a change in temperature (Table 2) than a change in density (Table 3). A larger variation is seen at the lower temperature range (300 eV to 1000 eV).

4. Effects of Stopping Power Models in Hydro-Simulations

All four models were implemented into the one-dimensional hydrocode, *LILAC*, as a subroutine using the FORTRAN programming language. *LILAC* is used to simulate implosions. The effects of the different stopping power models were examined on National Ignition Facility (NIF)-scale ignition implosions through hydro-simulations. Results output by *LILAC*, such as total neutron yield, neutron-averaged ion temperature, and gain (the ratio of output energy to input energy) were used for analysis.

Two simulations were performed to examine the four proposed models in terms of the output gain, neutron yields and ion temperature. The simulations have different adiabats, which is the ratio of plasma pressure to the Fermi degeneracy pressure. The adiabat is a measure of how cold the target is.

The cross section of the target used in the simulations is shown in Figure 4. The target is a spherical plastic (CH) capsule (37 μm thick) with a layer of 150 μm of deuterium-tritium (DT) ice, and is filled with three atmospheres of DT gas (radius of 1500 μm).

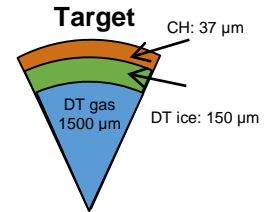


Figure 4: Cross section of the simulation target.

4.1 LILAC Simulation at a Moderate Adiabat ($\alpha=2$)

The first simulation was performed at a moderate adiabat ($\alpha=2$). A laser beam, with its pulse shape described in Figure 5a, is fired at the target. Figure 5b is the snapshot of density and ion temperature distributions in the target within the radius of 150 μm from the target center at 11.361 nanoseconds (soon after the beginning of the burn process) of the implosion. It is evident, as shown in Figure 5b, that there are large differences among the four models while the Skupsky model and LP model are nearly identical. Table 4 shows how the ion temperature differences affect the output performance.

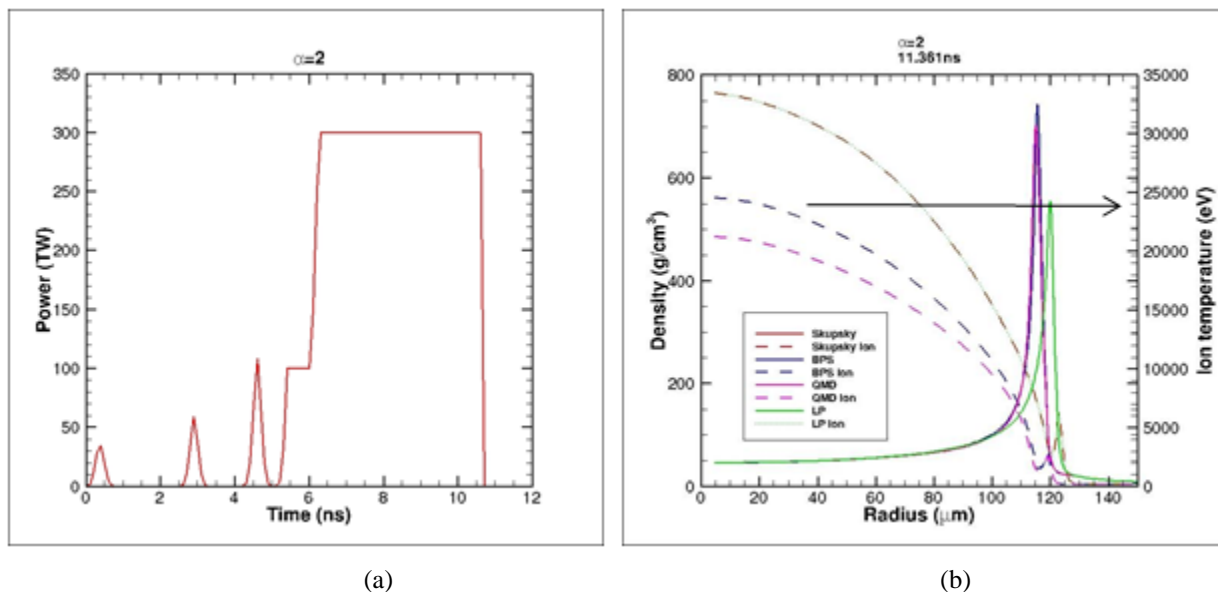


Figure 5: (a) Pulse shape in terms of power (TW) for the $\alpha=2$ design. (b) Snapshot of density (solid curves) and ion temperature (dotted curves) distributions at 11.361 nanoseconds (beginning of the burn process) of the implosion in the LILAC simulation at an adiabat of 2.0.

The goal of the NIF is to maximize the outputs (Table 4) of an implosion, especially the gain. The total neutron yield, ion temperature, and gain are important in determining the effectiveness of an implosion. In Table 4, the results of the different stopping power models show significant changes in the overall target performance, in which the target gain could vary by a factor of nearly two, 1.87 to be exact.

Outputs from simulation Moderate adiabat ($\alpha=2$)	BPS	LP	QMD	Skupsky
Total neutron yield	1.78E+19	2.35E+19	1.25E+19	2.35E+19
Neutron-averaged ion temperature	20.68 keV	28.88 keV	15.14 keV	28.88 keV
Gain (output energy/ input energy)	33.263	43.924	23.482	43.922

Table 4 The total neutron yield, the ion temperature, and the gain from all four models in the LILAC simulation at adiabat of 2.0.

4.2 LILAC Simulation at a Low Adiabat ($\alpha=1.7$)

In the second simulation, the same target shown in Figure 4 is used but in a low ($\alpha=1.7$) adiabat condition. In Figure 6a, the pulse shape for the low adiabat is different than that for the moderate adiabat. The low adiabat pulse is in a linear ramp shape. It is designed to avoid hot electron generation and electron preheating by slowly increasing the power.

Similar to moderate adiabat conditions, there are large differences in the density (solid lines) and ion temperature (dotted lines) distributions in the target among the models as shown in Figure 6b, while the Skupsky model and LP models are again nearly identical. In Table 5, the results show even larger changes in overall target performance, a difference by a factor of 2.66.

For both low and moderate adiabats, there are significant differences in the predictions of gain from the four stopping-power models that warrant further investigation. Accurate gain predictions allow for better nuclear fusion implosion experiments to be designed in the future. The gain from the implosion is the ultimate goal of nuclear fusion as an energy resource, so it is important to find a model that can accurately predict target performance.

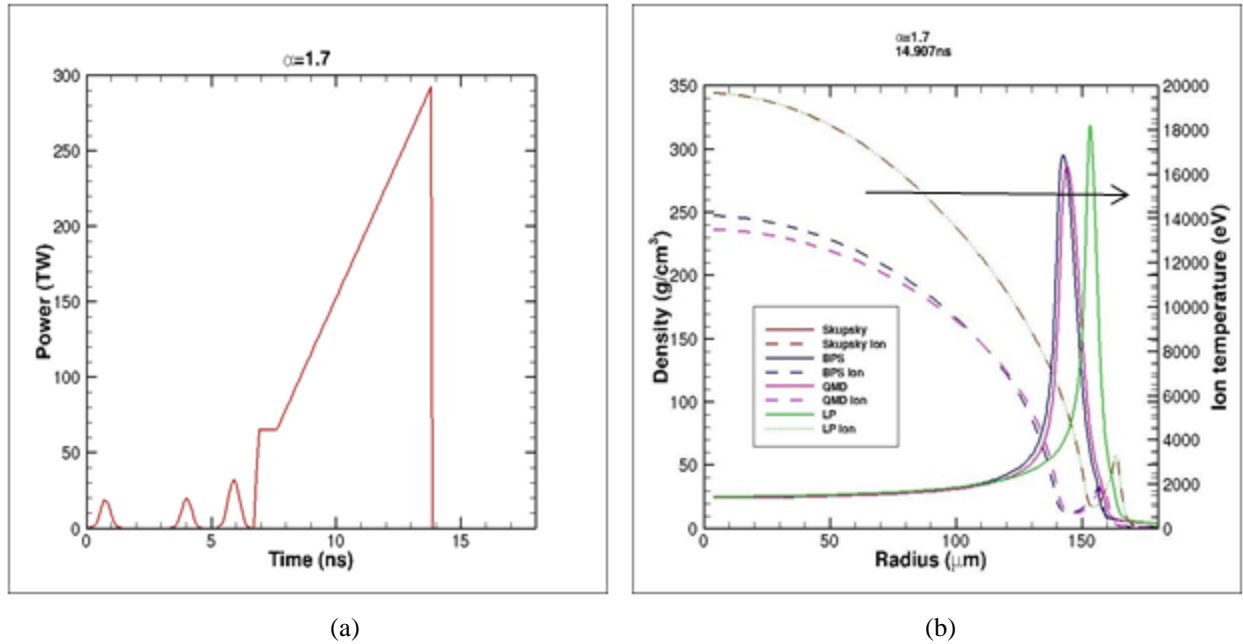


Figure 6: (a) Pulse shape in terms of power (TW). (b) Snapshot of density (solid lines) and ion temperature (dotted lines) distributions at 11.361 nanoseconds (soon after the beginning of the burn process) of the implosion in *LILAC* simulations at an adiabat of 1.7.

Outputs from simulation Moderate adiabat ($\alpha=1.7$)	BPS	LP	QMD	Skupsky
Total neutron yield	2.29E+18	5.64E+18	2.12E+18	5.64E+18
Neutron-averaged ion temperature	8.81 keV	11.95 keV	8.57 keV	11.95 keV
Gain (output energy/ input energy)	5.374	13.218	4.966	13.216

Table 5 The total neutron yield, the ion temperature, and the gain from all four models in the *LILAC* simulation at an adiabat of 1.7.

5. Suggested Future Validation Experiments

The *LILAC* simulations above, although representative of ICF implosions in terms of density and ion temperature levels, do not have testable conditions—as it is very hard to make uniform plasma under such conditions. More measurable plasma conditions are proposed, i.e., density= 1 g/cc and temperature=10 eV, which can be used to validate which one of the four stopping-power models best represents reality. Protons, which are more viable and manageable particles compared to alpha particles, are proposed for this experiment. The stopping power and distance traveled by a proton calculated from the four models are shown in Figure 7.

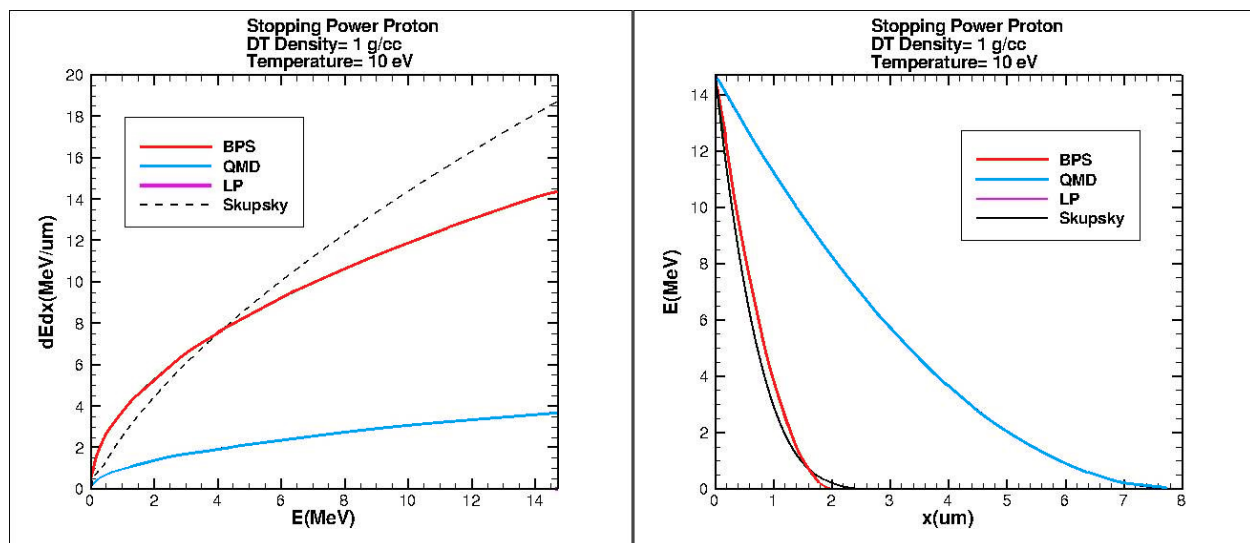


Figure 7: Calculated stopping power for a density of 1 g/cc and temperature of 10 eV

Stopping power is plotted as a function of proton particle energy in the left panel. The right panel shows how far the proton particle will travel in the plasma when the DT density is 1 g/cc and the temperature is 10 eV. On the left panel, the LP model predicts a stopping power curve that is very close to 0 MeV/ μm or negative; this makes the curve invisible. This translates into the LP model predicting a curve, on the right panel, that does not fit in the limits of the right panel.

In an ideal case, the actual physical measurements from this experiment would validate which stopping power model is the most accurate: there would be a model that closely coincides with the experiment's results. However, the actual physical measurements may not match any of the models. All in all, the experimental results may guide researchers in finding future improvements of stopping power models. But even so, being able to predict the stopping power at 1 g/cc and 10 eV does not necessarily allow one to validate models at 50 g/cc and 6 keV or 400 g/cc and 1 keV.

6. Conclusion

The stopping power models, Brown-Preston-Singleton (BPS), Li-Petrasso (LP), Quantum Molecular Dynamics (QMD), and Skupsky (currently used in LLE's hydro-codes), have been examined in ICF plasmas. These models have been tested for different deuterium-tritium (DT) plasma conditions such as temperature, density, and initial alpha particle energy. The four stopping power models vary due to the different physics in each model. The results have been analyzed for similarities, differences, and patterns between these four models. An important discovery is that these models show large differences in DT-shell conditions. The results show that as temperature increases, the distance traveled by an alpha particle increases—in other words, the average stopping power decreases.

The stopping power effects are further examined in hydro-simulations using the program *LILAC* to predict ICF performance. The results show significant changes in the overall target performance depending on which model is used; changes in target gain varied by a factor of two. Finally, a future experiment for testing the four models in measurable plasma conditions was suggested. This experiment could help determine if any of the models agree or closely coincide with experimental results.

Acknowledgements

I would like to thank Dr. S.X. Hu for being my research advisor for this project, Dr. R.S. Craxton for suggesting improvements, and the University of Rochester Laboratory for Laser Energetics for providing the resources to conduct my research.

References

1. S. Atzeni and J. Meyer-ter-Vehn, “The Physics of Inertial Fusion: Beam Plasma Interaction, Hydrodynamics, Hot Dense Matter,” International Series of Monographs on Physics (Clarendon Press, Oxford, 2004).
2. J. H. Nuckolls, L. Wood, A. Thiessen, and G. B. Zimmerman, “Laser Compression of Matter to Super-High Densities: Thermonuclear (CTR) Applications,” *Nature* 239, 139 (1972).
3. L.S. Brown, D. L. Preston, and R.L. Singleton, Jr., “Charged Particle Motion in a Highly Ionized Plasma,” *Phys. Rep.* 410, 237 (2005).
4. C.K. Li and R.D. Petrasso, “Charged-Particle Stopping Powers in Inertial Confinement Fusion Plasmas,” *Phys. Rev. Lett.* 70, 3059 (1993).
5. S. Skupsky, “Energy Loss of Ions Moving Through High-Density Matter,” *Phys. Rev. A* 36, 5701 (1987).
6. S.X. Hu, L.A. Collins, T.R. Boehly, J.D. Kress, V.N. Goncharov, and S. Skupsky, “First-Principles Thermal Conductivity of Warm-Dense Deuterium Plasmas for Inertial Confinement Fusion Applications,” *Phys. Rev. E* 89, 043105 (2014).
7. J. Delettrez, R. Epstein, M. C. Richardson, P. A. Jaanimagi, and B. L. Henke, “Effect of Laser Illumination Nonuniformity on the Analysis of Time-Resolved X-Ray Measurements in UV Spherical Transport Experiments,” *Phys. Rev. A* 36, 3926 (1987).
8. International Commission on Radiation Units and Measurements Report 73: “Stopping of Ions Heavier than Helium,” *Journal of the ICRU*, 5 No. 1 (2005), Oxford Univ.
9. International Commission on Radiation Units and Measurements (October 2011). “Fundamental Quantities and Units for Ionizing Radiation,” in Seltzer, Stephen M. *Journal of the International Commission on Radiation Units and Measurements* (Revised ed.) 11 (1).